Available online at www.sciencedirect.com
SCIENCE DIRECT®
International Journal of Heat and Mass Transfer 48 (2005) 1470–1479
International Journal of HEAT and MASS TRANSFER
www.elsevier.com/locate/ijhmt

Natural convection heat transfer in partially open inclined square cavities

E. Bilgen *, H. Oztop

Ecole Polytechnique, University of Montreal, C.P. 6079, 'centre ville', Montreal, QC, Canada H3C 3A7

Received 12 August 2004; received in revised form 21 October 2004
Available online 10 December 2004

Abstract

A numerical study has been carried out on inclined partially open square cavities, which are formed by adiabatic walls and a partial opening. The surface of the wall inside the cavity facing the partial opening is isothermal. Steady-state heat transfer by laminar natural convection in a two dimensional partially open cavity is studied by numerically solving equations of mass, momentum and energy. Streamlines and isotherms are produced, heat and mass transfer is calculated. A parametric study is carried out using following parameters: Rayleigh number from 10^3 to 10^6, dimensionless aperture size from 0.25 to 0.75, aperture position at high, center and low, and inclination of the opening from 0° (facing upward) to 120° (facing 30° downward). It is found that the volume flow rate and Nusselt number are an increasing function of Rayleigh number, aperture size and generally aperture position. Other parameters being constant, Nusselt number is a non-linear function of the inclination angle. Depending on the application, heat transfer can be maximized or minimized by selecting appropriate parameters, namely aperture size, aperture position and inclination angle at a given operation Rayleigh number.

Keywords: Natural convection; Partially open cavity; Inclined cavity

1. Introduction

Partially open cavities are encountered in various engineering systems, such as open cavity solar thermal receivers, uncovered flat plate solar collectors having rows of vertical strips, electronic cooling devices, in buildings, etc. A literature review shows that numerous studies have been published on a square open cavity. Excluding a series of experimental studies at a specific Rayleigh number, most of these studies has been with fully open horizontal cavities with all three isothermal walls or the wall facing the opening isothermal with the other two adiabatic. Since the fully open cavities represent a special case of the more general case considered in this study, we will present a brief review including fully open cavities.

Various authors studied experimentally open cavities [1–5]. The first two works were with horizontal fully open cavity [1,2]. The last three were with fully and partially open cavities [3–5]. The dimensionless aperture size in Hess and Henze [3] was 0.5 and it was centrally located in a square cavity. They used a laser Doppler velocimetry and flow visualization techniques to study

* Corresponding author. Tel.: +1 514 340 4711x4579; fax: +1 514 340 5917.
E-mail address: bilgen@polymtl.ca (E. Bilgen).

0017-9310/$ - see front matter © 2004 Elsevier Ltd. All rights reserved.
doi:10.1016/j.ijheatmasstransfer.2004.10.020

Nomenclature

A	enclosure aspect ratio, H/L
AP	dimensionless aperture position, d/H
AR	dimensionless aperture size, h/H
c_p	heat capacity, J/kg K
g	acceleration due to gravity, m/s^2
H	cavity height, m
k	thermal conductivity, W/m K
L	cavity width, m
Nu	Nusselt number, Eq. (5)
p	pressure, Pa
P	dimensionless pressure, $(p - p_\infty)L^2/\rho\alpha^2$
Pr	Prandtl number, v/α
Ra	Rayleigh number, $g\beta\Delta TL^3/(v\alpha)$
t	time, s
ΔT	temperature difference, $T - T_\infty$
U,V	dimensionless fluid velocities, uL/α, vL/α
$\dot{V}$	dimensionless volume flow rate through the opening
X,Y	dimensionless Cartesian coordinates, x/L, y/L
x,y	Cartesian coordinates

Greek symbols

α	thermal diffusivity, m^2/s
β	volumetric coefficient of thermal expansion, 1/K
v	kinematic viscosity, m^2/s
ρ	fluid density, kg/m^3
ψ	stream function
θ	dimensionless temperature, $(T - T_\infty)/(T_1 - T_\infty)$
φ	inclination angle of the heated wall from the horizontal, °
τ	dimensionless time, $\alpha t/L^2$

Superscripts

$\bar{}$	average

Subscripts

a	air
ext	extremum
f	fluid
in	into cavity
loc	local
max	maximum
min	minimum
out	out of cavity
∞	ambient value
1	hot wall

flow characteristics and determined local Nusselt number at various levels covering Rayleigh number from 10^7 to 10^{11} in laminar and turbulent regimes. Chakroun et al. [4] studied fully and partially open inclined cavities with aperture size from 0.25 to 1, aperture located centrally. Grashof number was 5.5×10^8 and constant. Later using the same experimental set-up, they studied the effect of the aperture location in an inclined square cavity with isothermal heated wall at the same Grashof number [5].

Others studied theoretically laminar natural convection heat transfer in fully open cavities [6–11]. Le Quere et al. [6] investigated thermally driven laminar natural convection in enclosures with all three sides isothermal, one of which facing the opening. Their range of Grashof was from 10^4 to 10^7. Penot [7] studied a similar problem using stream function-vorticity formulation. His Grashof range was 10^3–10^5. Chan and Tien [8] studied numerically a square fully open cavity, which had an isothermal vertical heated side facing the opening and two adjoining adiabatic horizontal sides. In these studies, the computation was done using an extended domain. Despite the difficulties due to unknown boundary conditions at the opening plane, the other studies mentioned above were undertaken using a computational domain restricted to the cavity. Chan and Tien [9] studied numerically shallow fully open cavities and also made a comparison study using a square cavity in an enlarged computational domain. They found that for a square open cavity having an isothermal vertical side facing the opening and two adjoining adiabatic horizontal sides, satisfactory heat transfer results could be obtained, especially at high Rayleigh numbers. In a similar way, Mohamad [10] studied inclined fully open square cavities, by considering a restricted computational domain. Different from those by Chan and Tien [9], gradients of both velocity components were set to zero at the opening plane. It was found that heat transfer was not sensitive to inclination angle and the flow was unstable at high Rayleigh numbers and small inclination angles. Polat and Bilgen [11] studied numerically inclined fully open shallow cavities in which the side facing the opening was heated by constant heat flux, two adjoining walls were insulated and the opening was in contact with a reservoir at constant temperature and pressure. The computational domain was restricted to the cavity. Miyamoto et al. [12] studied numerically partially and fully open square cavity with all three walls isothermal and various inclination angles. In case of partially open cavity, the dimensionless aperture size was 0.5 and it was

centrally located. Their Rayleigh number was from 0.7 to 7×10^5 for horizontal cavity and from 7×10^3 to 7×10^4 for inclined cavities. They used an extended computational domain.

Literature review shows that in the experimental studies with partially open cavities, either Rayleigh number was kept constant [4,5], or it was very high [3]. In the numerical study of the same problem, all three walls were heated [12]. In the present study, we will analyze and present results obtained from a numerical study of heat transfer by natural convection with ambient fluid at $Pr = 0.72$, at Rayleigh number from 10^3 to 10^6 using a computation domain restricted to partially open inclined cavity. Following applications encountered in thermal systems, the wall facing the opening is isothermal, and in contact with air in the open enclosure. All other walls are insulated. The ambient air at a characteristic temperature circulates through the opening dissipating heat from the hot wall by natural convection.

2. Problem and mathematical model

2.1. Problem definition

A schematic of the two dimensional system is shown in Fig. 1. The energy from the isothermal wall facing the opening is dissipated by convection of ambient fluid at T_∞ through the opening. The outer surfaces of the cavity are all insulated. The coordinate system and boundary conditions are also shown in Fig. 1. The cases considered are: three dimensionless aperture sizes, three dimensionless aperture positions, five inclination angles, 45 cases all.

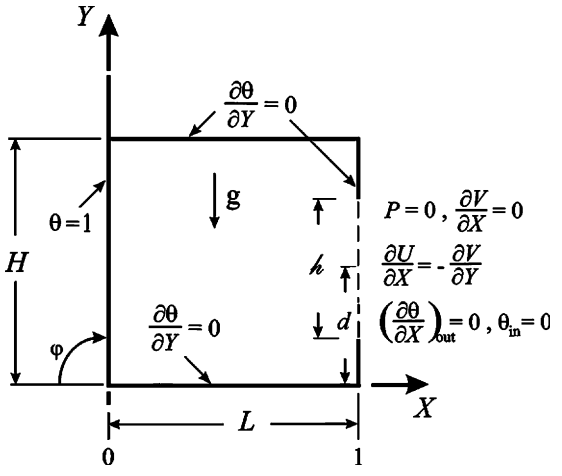

Fig. 1. Schematic of the open cavity system, the coordinate system and boundary conditions.

2.2. Mathematical model

The continuity, momentum and energy equations for a two dimensional laminar flow of an incompressible Newtonian fluid are written. Following assumptions are made: there is no viscous dissipation, the gravity acts in the vertical direction, fluid properties are constant and fluid density variations are neglected except in the buoyancy term (the Boussinesq approximation) and radiation heat exchange is negligible. Using non-dimensional variables defined in the nomenclature, the non-dimensional governing equations are obtained as

$$\frac{\partial U}{\partial X}+\frac{\partial V}{\partial Y}=0 \tag{1}$$

$$\frac{\partial U}{\partial \tau}+U\frac{\partial U}{\partial X}+V\frac{\partial U}{\partial Y}=-\frac{\partial P}{\partial X}+RaPr\theta\cos\varphi+Pr\nabla^2U \tag{2}$$

$$\frac{\partial V}{\partial \tau}+U\frac{\partial V}{\partial X}+V\frac{\partial V}{\partial Y}=-\frac{\partial P}{\partial Y}+RaPr\theta\sin\varphi+RaPr\theta+Pr\nabla^2V \tag{3}$$

$$\frac{\partial \theta}{\partial \tau}+U\frac{\partial \theta}{\partial X}+V\frac{\partial \theta}{\partial Y}=\nabla^2\theta \tag{4}$$

As will be explained later, the steady-state solutions are obtained from unsteady-state equations, Eqs. (1)–(4).

The local, average and normalized Nusselt numbers are calculated respectively as

$$\left.\begin{aligned} Nu_{\mathrm{loc}} &= \frac{-\frac{\partial\theta}{\partial X}}{\theta}\\ \overline{Nu} &= \int_0^A Nu_{\mathrm{loc}}\,\mathrm{d}Y\\ Nu &= \frac{\overline{Nu}_{Ra}}{\overline{Nu}_{Ra=0}} \end{aligned}\right\} \tag{5}$$

The volumetric flow rate is calculated as

$$\left.\begin{aligned} \dot{V} &= -\int_{X=1} U_{\mathrm{in}}\,\mathrm{d}Y\\ U_{\mathrm{in}} &= U_{X=1}\ \text{if}\ U_{X=1}<0\\ U_{\mathrm{in}} &= 0\ \text{if}\ U_{X=1}\geqslant 0 \end{aligned}\right\} \tag{6}$$

The stream function is calculated from its definition as

$$U=-\frac{\partial\psi}{\partial Y},\qquad V=\frac{\partial\psi}{\partial X} \tag{7}$$

where ψ is zero on the solid surfaces and the streamlines are drawn by $\Delta\psi=(\psi_{\max}-\psi_{\min})/n$ with n = number of increments.

2.3. Boundary conditions

The boundary conditions of the system shown in Fig. 1 are $U = V = 0$ on all solid surfaces, $\partial P/\partial n = 0$ on all solid surfaces at the outside boundaries, $P = 0$ on the opening. On the adiabatic boundaries, $\partial\theta/\partial n = 0$, and on the wall facing the opening, $\theta = 1$. The boundary

conditions on the opening adopted in this study are shown in Fig. 1 and by the following equations

$$\text{at } X = 1 \quad P = 0, \quad \frac{\partial V}{\partial X} = 0,$$
$$\frac{\partial U}{\partial X} = -\frac{\partial V}{\partial Y}, \quad \left(\frac{\partial \theta}{\partial X}\right)_{\text{out}} = 0, \quad \theta_{\text{in}} = 0 \tag{8}$$

3. Numerical technique

The numerical method used to solve Eqs. (1)–(4) is the SIMPLER (semi-implicit method for pressure linked equations revised) algorithm [13]. The computer code based on the mathematical formulation discussed earlier and the SIMPLER method were validated for various cases published in the literature, the results of which are discussed elsewhere [14].

Non-uniform grid in X and Y direction were used for all computations. Grid convergence was studied for the case of AR = 0.5 at center position and $\varphi = 90°$ with grid sizes from 20×20 to 60×60 at $Ra = 10^5$. Grid independence was achieved within 1.5% in Nusselt number and 0.55% in volume flow rate with grid size of 30×30. Similar tests were done with the cavities having different aperture size and inclination, and the grid sizes were adjusted accordingly. Using a system with 2.2 GHz clock speed, a typical execution time, at $Ra = 10^5$ for example, was 359 s.

The accuracy control was carried out by the conservation of mass by setting its variation to less than 10^{-3}, on the pressure term by setting the variation of residues at 10^{-3}. In addition, the accuracy of computations was checked using the energy conservation within the system, by setting its variation to less than 10^{-4}.

3.1. Validation

To validate the code, the case of a horizontal fully open square cavity having an isothermal wall reported by Chan and Tien [8] was studied. They used an extended computation domain and we used a computation domain restricted to the cavity. The results of comparison are presented in Table 1. We can see that the deviations vary from 22.4% for Nusselt number and 29.2% for flow rate at low Rayleigh number to 1.3% and 0.3% respectively at high Rayleigh number. The reason for the large deviations at low Rayleigh numbers is explained by the fact that the heat transfer is dominated by conduction regime and since the temperature at the opening is set at $\theta = 0$, the temperature gradient is higher, hence Nusselt number is higher than with enlarged computation domain case. This effect disappears gradually at high Rayleigh numbers as the heat transfer becomes convection dominated. Nevertheless, as shown earlier [15], the results obtained with computation domain restricted to the cavity will be acceptable for practical range of Rayleigh numbers considered in this study.

Table 1
Comparison of results with a horizontal fully open square cavity

Ra	Nu [8]	Nu (this study)	$\dot{V}$ [8]	$\dot{V}$(this study)
10^3	1.07	1.31	1.95	2.52
10^4	3.41	3.53	8.02	9.05
10^5	7.69	7.85	21.1	22.1
10^6	15.00	15.20	47.3	47.02

4. Results and discussion

Geometrical and thermal parameters governing the heat transfer and the flow rate in inclined partially open cavities are aspect ratio $A = L/H$, aperture size AR = h/H, opening position AP = d/H, inclination φ, and Ra, see Fig. 1. The geometrical cases are: three aperture sizes of 0.25, 0.50 and 0.75 located at center, high and low positions, nine in all.

Flow and temperature fields, heat transfer and volume flow rate through the cavity are examined for ranges of Rayleigh number from 10^3 to 10^6, the aspect ratio of $A = 1$, the aperture size AR = h/H of 0.25, 0.5 and 0.75, the aperture position AP = d/H at 0.125 (the lowest dimensionless position), 0.5 and 0.875 (the highest dimensionless position), and φ from 0° (the aperture facing upward) to 120° (the aperture facing 30° downward). All results are with $Pr = 0.72$. First, we will present temperature and flow fields for a square cavity with aperture size AR = 0.5, aperture position AP = 0.5, $\varphi = 90°$. Then we will present the same to see the effects of aperture size AR, aperture position AP and finally inclination angle φ. Following these observations, we will present the normalized Nu number and volume flow rate, $\dot{V}$, both as a function of Rayleigh number and the other non-dimensional parameters.

4.1. Temperature and flow fields

Isotherms and streamlines for the case with $A = 1$, AR = $h/H = 0.5$, AP = $d/H = 0.5$, $\varphi = 90°$ are presented in Fig. 2 for Rayleigh number from 10^3 to 10^6. We observe in Fig. 2(a) that the heat transfer in the cavity is quasi-conductive at $Ra = 10^3$ and becomes dominated by convective regime as Ra increases to 10^6 in Fig. 2(b)–(d). At $Ra = 10^3$, the streamlines in the cavity show that for quasi-conductive regime the entrance and exit sections of the fluid at the opening are almost equal. $|\Psi_{\text{ext}}| = 1.17$ at $X = 0.58$, $Y = 0.48$. At $Ra = 10^4$ in Fig. 2(b), the heat transfer is by conduction as well as convection: $|\Psi_{\text{ext}}| = 5.59$ at $X = 0.53$, $Y = 0.50$, showing clearly

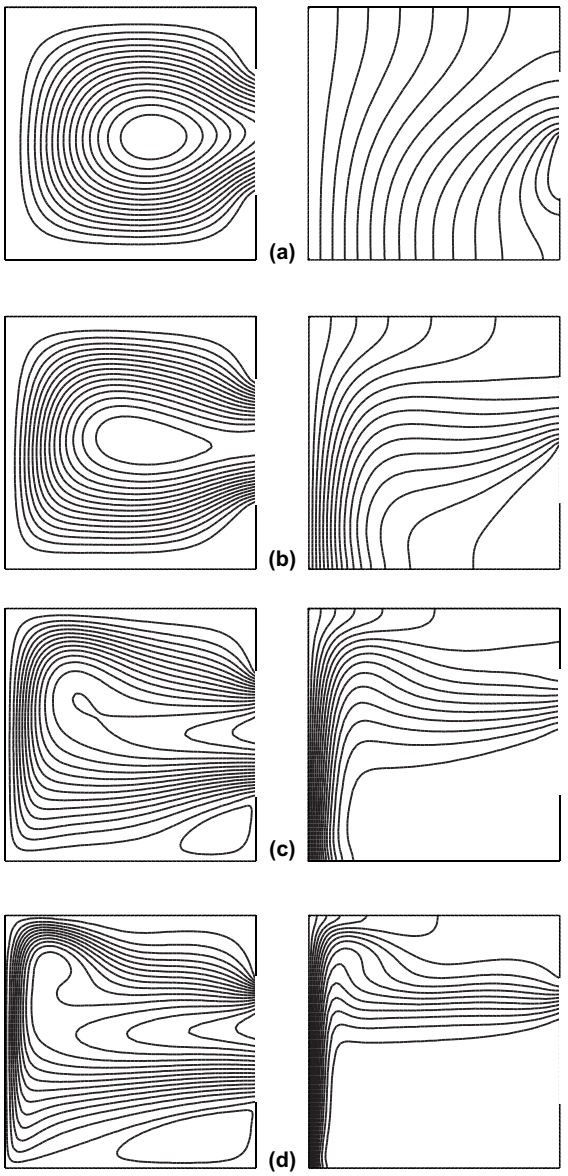

Fig. 2. Flow (on the left) and temperature (on the right) fields for the case AR = $h/H = 0.50$, AP = $d/H = 0.50$, $\varphi = 90°$ (a) $Ra = 10^3$, (b) $Ra = 10^4$, (c) $Ra = 10^5$, (d) $Ra = 10^6$.

the increased contribution of convection. The isotherms show formation of a boundary layer heat transfer along the hot wall. As Ra increases to 10^5, Fig. 2(c) shows that a convective regime is established: the cold fluid entrained through the larger section of the opening moves across the cavity following the lower bounding wall, rises along the hot wall, moves across the upper part following the top bounding wall and discharges at the opening. A convection cell is formed at the lower right corner as the fluid accelerates toward the hot wall and the larger circulating convection cell is not symmetric with $|\Psi_{ext}| = 16.19$ at $X = 1$, $Y = 0.51$. The isotherms show a boundary layer heat transfer and a cold region corresponding to the second convection cell at the right lower corner. At $Ra = 10^6$, $|\Psi_{ext}| = 33.86$ at $X = 1$, $Y = 0.57$, which shows a similar trend to the case with $Ra = 10^5$, with enhanced convection and boundary layer flow and heat transfer at the hot wall, enlarged secondary convection cell at the right lower corner. The flow of warm fluid is confined to the boundary layer and upper half of the cavity and the lower part of the cavity filled with cold fluid. We see that as Ra increases, the flow becomes fully convection dominated, the cold fluid is entrained right to the hot wall where high temperature gradients are created, and the discharging fluid from the upper part of the cavity occupies smaller and smaller section of the opening, being a jet like at high Rayleigh numbers.

The effect of aperture size AR = h/H is presented in Fig. 3, for AP = 0.50, $Ra = 10^5$, $\varphi = 90°$ with AR = $h/H = 0.25$ (smaller opening) and 0.75 (larger opening). The case for AR = 0.50 is shown in Fig. 2(c). We can see that as expected the cold fluid's acceleration is higher for AR = $h/H = 0.25$ and smaller for AR = $h/H = 0.75$, otherwise similar trends exist. $|\Psi_{ext}| = 11.35$ at $X = 0.65$, $Y = 0.39$ for AR = $h/H = 0.25$ in Fig. 3(a) and $|\Psi_{ext}| = 18.90$ at $X = 1$, $Y = 0.608$ for AR = $h/H = 0.75$, in Fig. 3(b). We see that convection is enhanced with larger opening and the reverse is the case for smaller opening, a trend which may be expected since the resistance to flow in and out the cavity will be smaller in the former case.

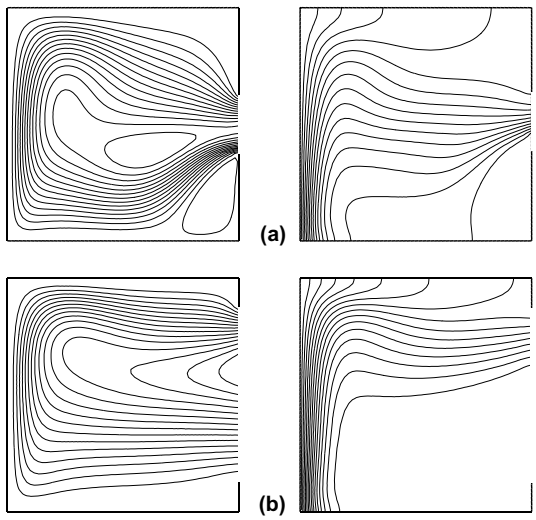

Fig. 3. Flow (on the left) and temperature (on the right) fields for the case AP = $d/H = 0.50$, $\varphi = 90°$ and $Ra = 10^5$ (a) AR = $h/H = 0.25$, (b) AR = $h/H = 0.75$.

The effect of the position of the opening is presented in Fig. 4, for AR = 0.50, $Ra = 10^5$, $\varphi = 90°$ with AP = $d/H = 0.75$ (high position) and 0.25 (low position). The case for AP = 0.50 is shown in Fig. 2(c). These two correspond to upper and lower half openings respectively. We can see in Fig. 4(a) that the cold fluid enters the cavity at the lower part of the opening, accelerates to the hot wall leaving right lower part of the cavity where a secondary convection cell is formed. $|\Psi_{ext}| = 19.29$ at $X = 1.0$, $Y = 0.736$ for the main circulation and $|\Psi| = 2.23$ at $X = 0.68$, $Y = 0.26$ for the secondary cell. The isotherms show that the entire right lower part of the cavity remains cold. Fig. 4(b) shows the case with AP = 0.25 in which case the air enters the cavity similarly at the lower part of the opening and flows parallel to the lower wall, heated up at the hot wall all the way up the top and exit at the upper part of the opening. The fluid sweeps the entire cavity except the right upper corner. $|\Psi_{ext}| = 24.96$ at $X = 0.5$, $Y = 0.5$. The isotherms show that the upper right corner of the cavity remains cold. In comparing results in Fig. 2(c) and Fig. 4(a) and (b), it appears that all the parameters being the same, at the low aperture position the convection is highest, as a result of which heat transfer should be better. Between the center and high positions, the convection is stronger in high positioned aperture.

The effect of inclination is presented in Fig. 5 for AR = AP = 0.50, $Ra = 10^5$ with $\varphi = 30°$, 60° and 120° angles. The case for $\varphi = 90°$ is shown in Fig. 2(c). $\varphi = 30°$ shown in Fig. 5(a) corresponds to the upward facing opening in which the convection is quasi-symmetric with $|\Psi_{ext}| = 35.00$ at $X = 0.55$, $Y = 0.50$. The convection strength is almost double that of case $\varphi = 90$ in Fig. 2(c). The isotherms indicate a boundary layer flow at the hot wall. This is expected since the cold fluid enters the cavity added by the gravity and the hot fluid exits almost vertically. The case with $\varphi = 60°$ shown in Fig. 5(b) has almost the same appearance as that of Fig. 5(a), except a secondary cell is formed at the right lower corner and the main cell is not symmetric, $|\Psi_{ext}| = 39.36$ at $X = 0.51$, $Y = 0.50$ with stronger circulation in the cavity. In contrast, the case with $\varphi = 120°$ shown in Fig. 5(c) has $|\Psi_{ext}| = 7.96$ at $X = 1$, $Y = 0.53$, i.e. considerably reduced circulation strength and a non-symmetric cell. The isotherms indicate quasi-conductive regime at the lower and upper boundaries and heat transfer at the lower part of the hot wall. This is also expected since the opening is facing downward for this case.

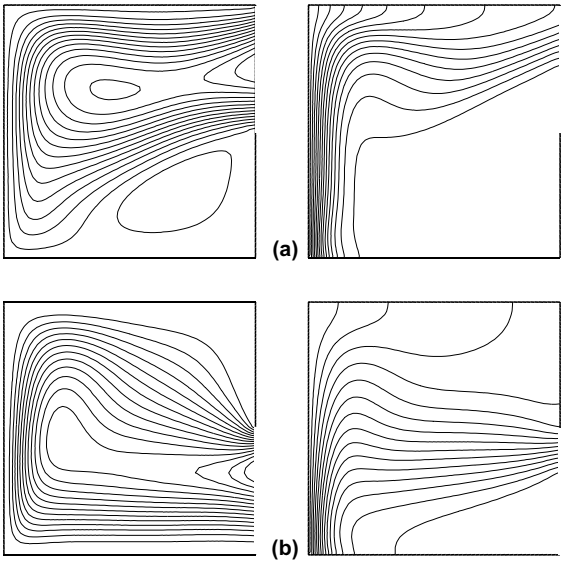

Fig. 4. Flow (on the left) and temperature (on the right) fields for the case AR = $h/H = 0.50$, $\varphi = 90°$, $Ra = 10^5$, (a) AP = $d/H = 0.75$, (b) AP = $d/H = 0.25$.

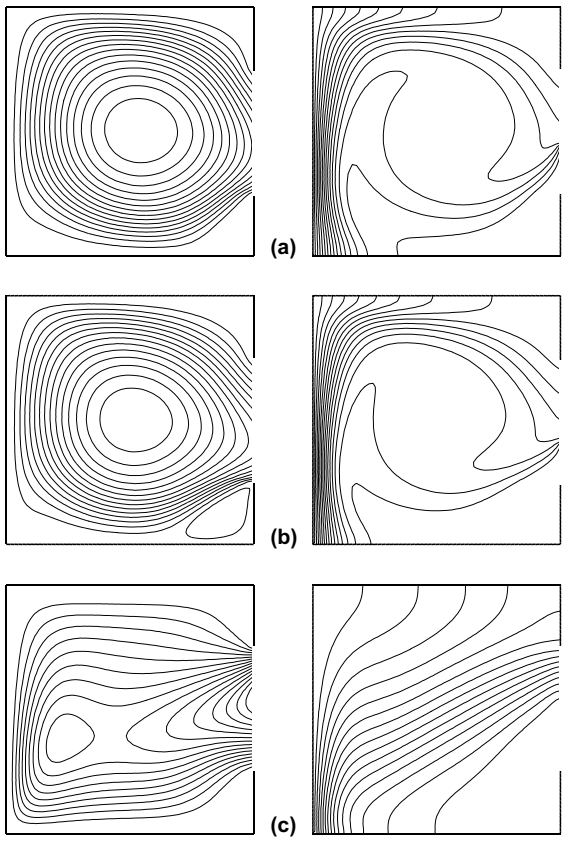

Fig. 5. Flow (on the left) and temperature (on the right) fields for the case AR = $h/H = 0.50$, AP = $d/H = 0.50$, $Ra = 10^5$ for various inclination angles, (a) $\varphi = 30°$, (b) $\varphi = 60°$, (c) $\varphi = 120°$.

4.2. Temperature and velocity profiles

Non-dimensional temperature and velocity profiles at the opening and mid-planes are presented in Fig. 6 for

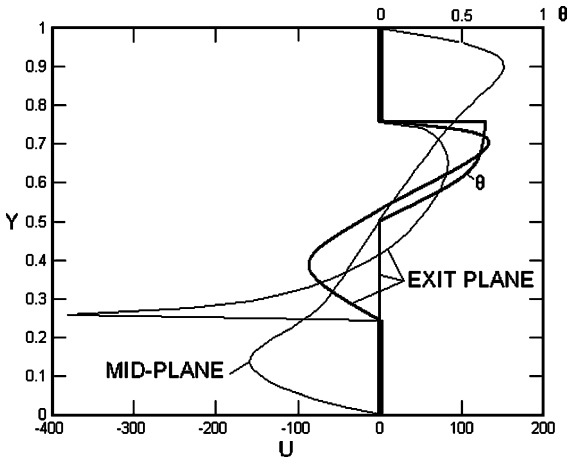

Fig. 6. Velocity and temperature profiles at exit plane for AR = AP = 0.50, $Ra = 10^5$ and $\phi = 90°$ (shown with thick lines), and velocity profiles at mid-plane and exit plane for the case AR = AP = 0.50, $Ra = 10^5$ and $\phi = 60°$ (shown with thin lines).

the case AR = AP = 0.5, $Ra = 10^5$. Velocity and temperature profiles for $\varphi = 90°$ are shown with thick lines while velocity profiles at mid-plane and exit plane for $\varphi = 60°$ with thin lines. We can see that for the horizontal case with $\varphi = 90°$, the velocity profile at the exit plane is almost symmetric, the fluid enters the cavity at temperature $\theta = 0$ and exits at a temperature increasing in the Y direction, as expected from earlier observations. The incoming and outgoing flows occupy the aperture area unequally: 53.57% incoming flow and 46.43% outgoing flow. As a result, the maximum jet velocity of incoming flow is only 72.5% of that outgoing flow. Velocity profile at the exit for $\varphi = 60°$ shows that the incoming flow occupies 34.09% of the aperture area while the outgoing flow 65.91%, as a result of which the maximum jet velocity for the former is high and that of the latter is only 21.88% of it. At mid-plane the velocity profile is almost symmetric as expected, which was also observed earlier with the streamlines of Fig. 2.

4.3. Heat transfer and volume flow rate

We will present first volume flow rate, $\dot{V}$ and heat transfer, Nu as a function of Rayleigh number, Ra from 10^3 to 10^6 for various inclinations, φ from 0° to 120° for the case of centrally located apertures. Then we will present the effect of high and low positioning of apertures. We note that $\varphi = 90°$ corresponds to horizontal position of the cavity as shown in Fig. 1.

We present $\dot{V}$ and Nu as a function of Ra for centrally located aperture of 0.50 in Fig. 7. We see that the flow rate increases rapidly with increasing Ra up to 10^4 thereafter tapers off. $\dot{V}$ is generally higher when the

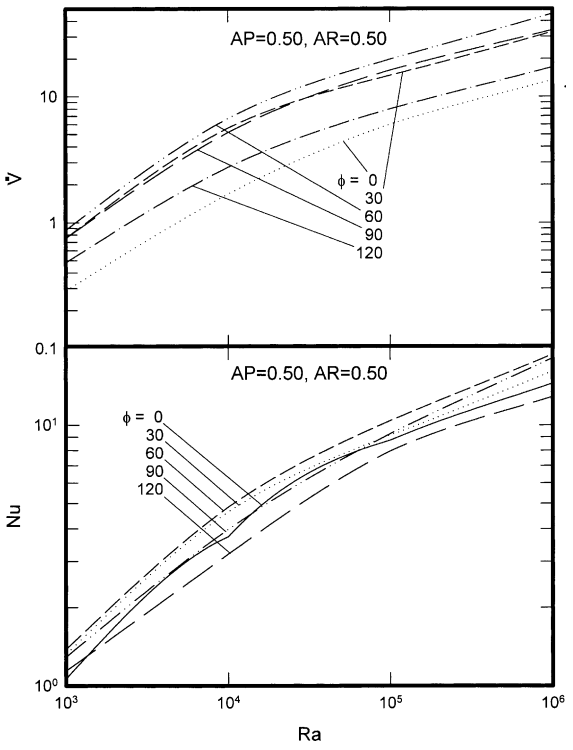

Fig. 7. Volume flow rate, $\dot{V}$ and normalized Nu number as a function of Ra with φ as a parameter for the case of AP = $d/H = 0.50$, AR = $h/H = 0.50$.

cavity aperture facing up and lowest when horizontal and/or facing down, an expected result due to geometrical position of the aperture. Nu variation with Ra follows a similar trend to that for $\dot{V}$, but heat transfer is higher for $\varphi = 60°$ and 30°, i.e. when the aperture is facing upward with an angle and lowest when facing downward with an angle. As observed with Fig. 2, at low Ra, heat transfer is conduction dominated and becomes convection dominated for $Ra > 10^4$. We note also in Fig. 7 that the convergence to a steady solution was achieved with difficulty for $\varphi = 0°$, i.e. up facing aperture case at $Ra \geqslant 10^5$ due to unstable flow conditions.

Similar results are presented for the case of centrally located aperture of AR = $h/H = 0.75$ in Fig. 8. As expected we observe with respect to the results in Fig. 7, increased flow rates at all inclinations due to larger aperture with less resistance to flow. Again the highest flow rate is at inclinations $\varphi = 60°$ and 30° and the lowest in the case aperture facing downward.

The results with aperture of 0.25 centrally located are presented in Fig. 9 for $\dot{V}$ and Nu. In this case, although the general trend for both $\dot{V}$ and Nu is similar to the case with 0.50 aperture size, due to relatively smaller aperture, the flow rate as well as heat transfer is proportionately reduced.

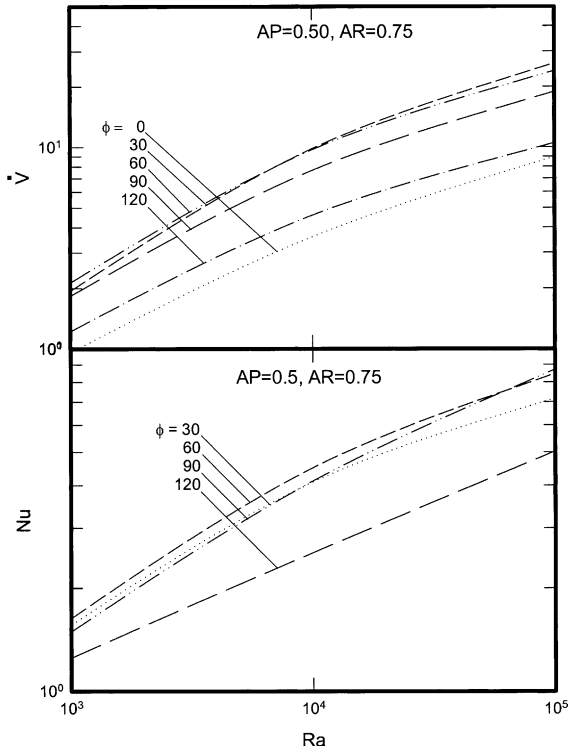

Fig. 8. Volume flow rate, $\dot{V}$ and normalized Nu number as a function of Ra with φ as a parameter for the case of AP = d/H = 0.50, AR = h/H = 0.75.

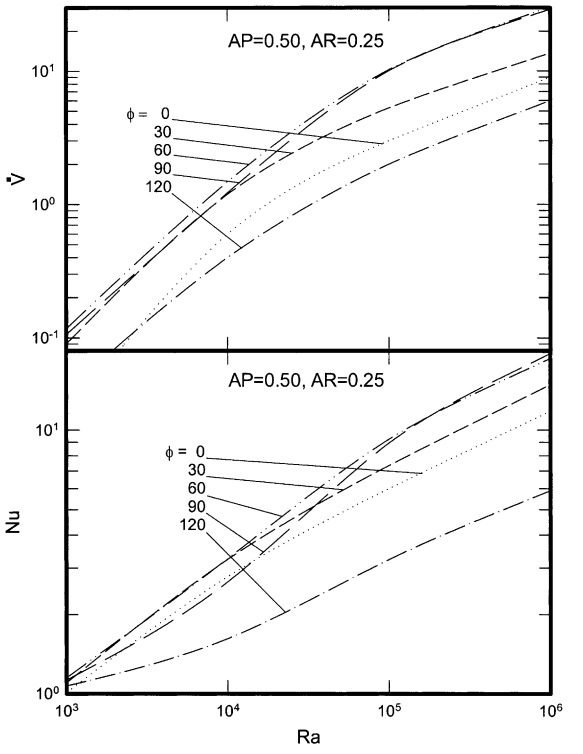

Fig. 9. Volume flow rate, $\dot{V}$ and normalized Nu number as a function of Ra with φ as a parameter for the case of AP = d/H = 0.50, AR = h/H = 0.25.

Fig. 10 shows a cross plot of the results for AP = 0.5 presented as Nusselt as a function of inclination angle, φ from 0° to 120° with Rayleigh as a parameter. Generally, Nusselt number shows a non-linear variation with increasing inclination, φ. It is relatively low at $\varphi = 0$, it starts increasing with φ, it goes through a maximum and decreases until φ reaches 120°. For $Ra = 10^3$, i.e. conduction dominated regime, Nusselt number increases with aperture size AR at all inclination, which is an expected result. Following the observations made for Figs. 2–4 as Rayleigh increases, a mixed situation arises with Nusselt having a higher value at different AR values at a given inclination angle, φ. Generally, at low φ, the heat transfer is higher for AR = 0.50 and at high φ, it is lower with respect to other apertures. For $Ra = 10^4$ and low φ, Nu is lowest for AR = 0.25 and highest for AR = 0.50, and in between for AR = 0.75. At $\varphi > 80°$ Nu is higher for AR = 0.75 than 0.50. For $Ra = 10^5$, Nu is highest for AR = 0.50 at all inclinations; at φ = 0–30°, it is higher for AR = 0.25 than 0.75 but it changes at $\varphi \approx 40°$ and once again at ≈90°.

Similar plots for AP = 0.75 and AP = 0.25 showed that for $Ra = 10^3$, the trend was the same as in the case with AP = 0.50. At convection dominated conditions, the differences were less striking, except at φ from 60° to 120°: for AP = 0.75, heat transfer was highest for AR = 0.75 except at $\varphi = 120°$ and for AP = 0.25, it was highest for AR = 0.50 except at $\varphi = 120°$. In comparing these plots we could clearly see that the heat transfer was generally better for low positioned apertures, which we have observed earlier with Figs. 2–5.

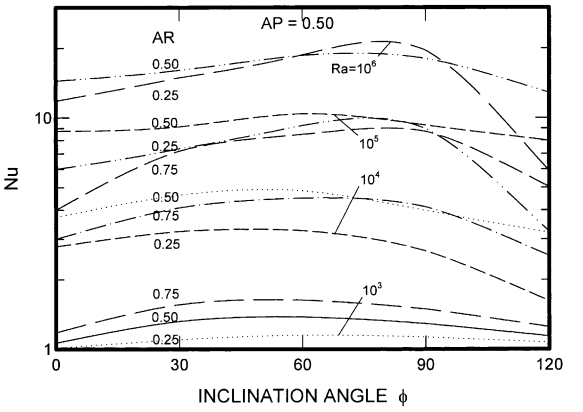

Fig. 10. Normalized Nu number as a function of the inclination angle, φ with Ra and AR = h/H as parameters and AP = d/H = 0.50.

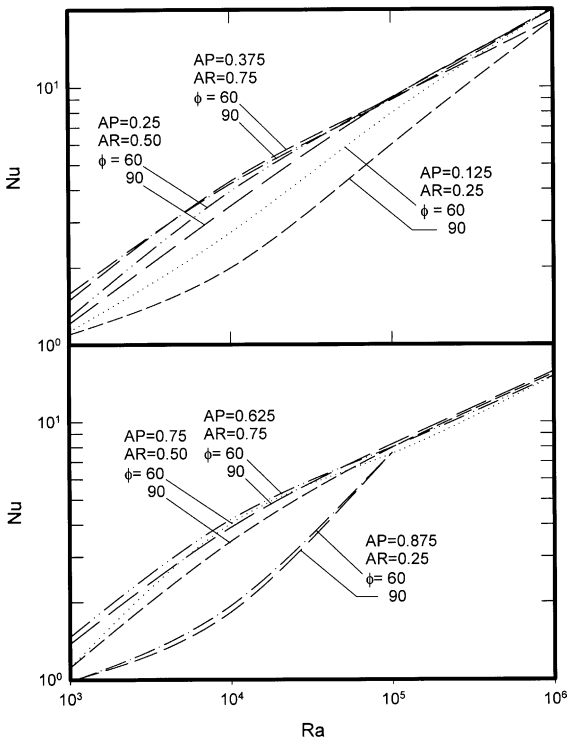

Fig. 11. Effects of aperture position AP = d/H and of aperture size AR = h/H on normalized Nu as a function of Ra at various inclinations φ. The upper figure is for low aperture position while the lower one is for high aperture position.

Effects of aperture position AP = d/H and of aperture size AR = h/H on normalized Nu as a function of Ra at various inclinations φ are shown in Fig. 11. The low aperture position is shown in the upper part of Fig. 11 while the high aperture position in the lower part. They should be compared with Fig. 7 for AP = 0.50. Following our observations in Figs. 2 and 4, the heat transfer at low Rayleigh numbers is almost the same for all three cases and we can see only a small effect of the aperture position, if any. At Rayleigh numbers from 10^5 to 10^6, as expected the heat transfer is higher when the aperture position is low with respect to that high, and following our observations regarding Figs. 4 and 2(c), it is higher when the aperture is positioned high with respect to that positioned at the center. This is also generally the case for various other inclination angles.

5. Conclusions

Steady-state heat transfer by natural convection in partially open inclined square cavities has been numerically studied. The cavity was formed by adiabatic walls, an isothermal wall facing the partial opening and it was inclined from 0°, i.e. the aperture facing upwards, to 120°, i.e. facing 30° downward. Rayleigh number was from 10^3 to 10^6, which covered a range not encountered in the previous studies [3–5].

Based on the findings in this study, we conclude that $\dot{V}$ and Nu are an increasing function of Ra, AR = h/H and generally of AP = d/H. The relationship between heat transfer, Nu and the inclination angle, φ is non-linear. Nu is maximized at 30–60° for low Rayleigh numbers and at 60–90° at high Rayleigh numbers. Depending on the application, which may require maximizing or minimizing of heat transfer through the aperture, the aperture size, AR, its position, AP and the inclination angle, φ should be chosen as design parameters. For example, at convection dominated conditions, for solar receiver applications, smaller aperture at center position and inclination angle from 90° to 120° would help minimize losses. On the other hand, for electronic cooling applications, large aperture at low position and inclined at 60–90° would maximize heat transfer. We have seen that depending on the Rayleigh number, these parameters can be different, thus the design parameter selection should be done for each specific case.

Acknowledgment

Financial support by Natural Sciences and Engineering Research Council of Canada is acknowledged.

References

[1] V. Sernas, I. Kyriakides, Natural convection in an open cavity, in: Proc. the Seventh Int. Heat Transfer Conf., Munich, 2, 1982, pp. 275–286.
[2] Y.L. Chan, C.L. Tien, Laminar natural convection in shallow open cavities, J. Heat Transfer 108 (1986) 305–309.
[3] C.F. Hess, R.H. Henze, Experimental investigation of natural convection losses from open cavities, J. Heat Transfer 106 (1984) 333–338.
[4] W. Chakroun, M.M. Elsayed, S.F. Al-Fahed, Experimental measurements of heat transfer coefficient in a partially/fully opened tilted cavity, J. Solar Eng. 119 (1997) 298–303.
[5] M.M. Elsayed, W. Chakroun, Effect of aperture geometry on heat transfer in tilted partially open cavities, J. Heat Transfer 121 (1999) 819–827.
[6] P. Le Quere, J.A.C. Humphrey, F.S. Sherman, Numerical calculation of thermally driven two-dimensional unsteady laminar flow in cavities of rectangular cross section, Numer. Heat Transfer 4 (1981) 249–283.
[7] F. Penot, Numerical calculation of two-dimensional natural convection in isothermal open cavities, Numer. Heat Transfer 5 (1982) 421–437.
[8] Y.L. Chan, C.L. Tien, A numerical study of two-dimensional natural convection in square open cavities, Numer. Heat Transfer 8 (1985) 65–80.

[9] Y.L. Chan, C.L. Tien, A numerical study of two-dimensional laminar natural convection in shallow open cavities, Int. Heat Mass Transfer 28 (1985) 603–612.
[10] A.A. Mohamad, Natural convection in open cavities and slots, Numer. Heat Transfer 27 (1995) 705–716.
[11] O. Polat, E. Bilgen, Laminar natural convection in inclined open shallow cavities, Int. J. Thermal Sci. 41 (2002) 360–368.
[12] M. Miyamoto, T.H. Kuehn, J. Goldstein, Y. Katoh, Two-dimensional laminar natural convection heat transfer from a fully or partially open square cavity, Numer. Heat Transfer A 15 (1989) 411–430.
[13] S.V. Patankar, Numerical Heat Transfer and Fluid Flow, Hemisphere, New York, 1980.
[14] R. Ben Yedder, E. Bilgen, Laminar natural convection in inclined enclosures bounded by a solid wall, Heat and Mass Transfer 32 (1997) 455–462.
[15] O. Polat, E. Bilgen, Conjugate heat transfer in inclined open shallow cavities, Int. J. Heat Mass Transfer 46 (2003) 1563–1573.